THE JOURNAL OF PHYSICAL CHEMISTRY A

Article

pubs.acs.org/JPCA

Nonadiabatic Photodynamics of a Retinal Model in Polar and Nonpolar Environment

Matthias Ruckenbauer,[†,⊥] Mario Barbatti,*[,‡] Thomas Müller,[§] and Hans Lischka*[,†,∥]

[†]Institute for Theoretical Chemistry, University of Vienna, Währingerstraße 17, 1090 Vienna, Austria

[‡]Max-Planck-Institut für Kohlenforschung, Kaiser-Wilhelm-Platz 1, 45470 Mülheim, Germany

[§]Forschungszentrum Jülich, Institute for Advanced Simulation, 53425 Jülich, Germany

[∥]Department of Chemistry and Biochemistry, Texas Tech University, Lubbock, Texas 79409-1061, United States

Supporting Information

ABSTRACT: The nonadiabatic photodynamics of the *all-trans*-2,4-pentadieneiminium cation (protonated Schiff base 3, PSB3) and the *all-trans*-3-methyl-2,4-pentadiene-iminium cation (MePSB3) were investigated in the gas phase and in polar (aqueous) and nonpolar (*n*-hexane) solutions by means of surface hopping using a multireference configuration-interaction (MRCI) quantum mechanical/molecular mechanics (QM/MM) level. Spectra, lifetimes for radiationless deactivation to the ground state, and structural and electronic parameters are compared. A strong influence of the polar solvent on the location of the crossing seam, in particular in the bond length alternation (BLA) coordinate, is found. Additionally, inclusion of the polar solvent changes the orientation of the intersection cone from sloped in the gas phase to peaked, thus enhancing considerably its efficiency for deactivation of the molecular system to the ground state. These factors cause, especially for MePSB3, a substantial decrease in the lifetime of the excited state despite the steric inhibition by the solvent.

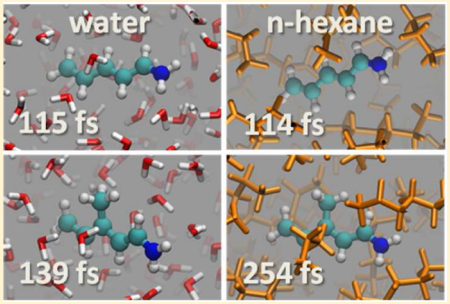

1. INTRODUCTION

The photodynamical behavior of retinal protonated Schiff bases (RPSBs) is of great interest, as they form the photoactive moiety in the family of rhodopsines.[1−5] When electronically excited, they perform an isomerization around a formal double bond within the limited range of the cavity of the opsine.[4−9] The class of protonated Schiff bases with *n* double bonds (PSB*n*, $H_2C{=}CH(CH{=}CH)_{n-2}CH{=}NH_2^+$) has been used extensively as models for studying the behavior of rhodopsines.[10−18] From this class of compounds, the 2,4-pentadieneiminium cation (PSB3) has been widely used as a model system showing many characteristic features of the larger chains.[10,13,15,18−22] In minimum energy path[10] and dynamics[15,18] studies, it has been shown that in the gas phase, after electronic excitation from the closed shell (π^2) ground state into the first excited ($\pi\pi^*$) state, PSB3 starts with an adaptation of the bond lengths to those of the excited state and continues with a torsion around the central CC bond. This deformation simultaneously stabilizes the excited state and destabilizes the ground state until it leads to a crossing seam between the two electronic surfaces. PSB3 has also been used in several recent studies to investigate the effect of dynamic electron correlation on conical intersections,[23] on reaction paths in the S_1 state[24] and on different reaction paths in the electronic ground state.[25] Furthermore, it has been chosen as a benchmark example to test the influence of zero point and classical sampling techniques on the semiclassical photodynamics.[26]

Most of these investigations have been performed for the isolated PSB*n*'s, concentrating on the characterization of static properties in ground and excited state,[10,12−14,19,20,22] but also the mechanisms of the photodynamical deactivation to the electronic ground state have been investigated in detail.[15,16,18] Embedding a chromophore into an environment enhances the complexity of the system considerably and may increase the required computational cost significantly. Probably the most popular strategy to arrive at manageable cost while keeping an explicit atomistic description is the hybrid quantum mechanical/molecular mechanical (QM/MM) approach, separating the entire molecular system into regions that can be computed by means of high levels of theory and a surrounding treated by molecular mechanics.[27−29]

Theoretical studies on PSB3 in condensed matter have dealt with questions such as the analysis of UV spectra or with the general description of solvent effects on the potential energy surfaces.[11,20,30−35] Additionally, investigations using nonadiabatic excited-state dynamics in combination with a QM/MM approach have become available in the past years.[5,36−44] In particular, a hybrid surface hopping scheme treating nonadiabatic dynamics with solvent effects and utilizing at the same time a full incorporation of ab initio quantum mechanical nonadiabatic couplings has been recently introduced by us into

Received: January 13, 2013
Revised: March 7, 2013
Published: March 7, 2013

   dx.doi.org/10.1021/jp400401f | *J. Phys. Chem. A* 2013, 117, 2790−2799

the Newton-X[16,45] program and applied to various photodynamical problems such as the PSB3 dynamics in nonpolar environment,[46] the photodecay of nucleobases in DNA environment models,[47−49] and the photodissociation of formamide within a frozen argon cavity.[50]

As concerns polar solvents, the electronic properties of PSB*n*'s are known to be altered considerably by electrostatic interactions with the environment, leading to a blue shift in the absorption spectra.[12] Such modifications are expected to show also a significant influence on the excited state deactivation dynamics as has been discussed in model calculations by Burghardt and Hynes.[31,51,52] To study these effects explicitly, the photodynamics of *all-trans*-PSB3 (Figure 1, left panel) was

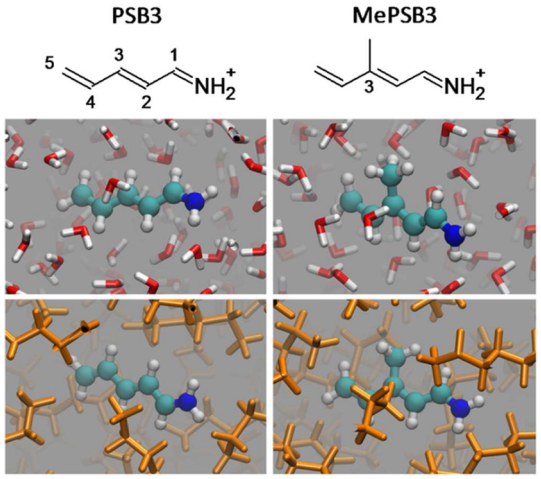

Figure 1. PSB3 (left portion) and MePSB3 (right portion) with numbering of carbon atoms and snapshots embedded in water and *n*-hexane, respectively.

investigated in this work for polar (aqueous) solution and for comparison reasons also for the gas phase and nonpolar (*n*-hexane) environment. It had been shown in our recent photodynamics study of PSB3 in nonpolar solution[46] that because of its structural flexibility, PSB3 is not strongly affected in its excited state motion by steric hindering of the solvent. Therefore, the methyl-PSB3 (3-methylpenta-2,4-diene-1-iminium cation, MePSB3) (Figure 1, right panel) had been included in the previous study in order to introduce a stronger variability in steric requirements. It has been shown that the CH_3 group reaching out from the molecule acts as a steric "anchor" in the solvent, hindering the torsion of the molecule significantly. Thus, MePSB3 is a good additional model system and will be investigated in our present study as well. A general multireference configuration-interaction (MRCI) approach[53] to describe the excited states will be used allowing the inclusion of several excited states at a high quantum chemical level and to perform full nonadiabatic dynamics studies in full generality.

2. COMPUTATIONAL DETAILS

2.1. QM/MM Ansatz. An electrostatic embedding QM/MM scheme was used separating the complete system of PSB3 and solvent into two subsets of atoms, an inner (I) and an outer region (O). Inner and outer regions are described by quantum mechanics and molecular mechanics, respectively. Specifically, multireference electronic structure methods are used to accurately describe multiple electronic states of the compound of interest, while the MM component primarily deals with environmental effects. Standard parametrized force fields are employed in the MM part incorporating bonded terms (bond stretching, angle bending, proper and improper torsions), van der Waals interactions (Lennard-Jones type potential), and electrostatic interaction between partial point charges associated with each atom. The total energy of the entire system (S) is given by

$$E_{QM/MM}(S) = E_{QM}(I) + E^{el}(I,O) + E_{MM}^{vdW}(I,O) + E_{MM}^{b+vdW}(O) + E_{MM}^{el}(O) \quad (1)$$

where the superscripts denote bonding (b), van der Waals (vdW), and electrostatic (el) interactions. An electrostatic embedding scheme is used in which the effective point charges of the atoms of the solvent molecules are included in the quantum mechanical Hamiltonian. More details of the technical aspects of the implementation can be found in ref 46.

Multireference configuration interaction including single excitations from the reference space (MR-CIS) based on a state-averaged (SA) complete active space self-consistent field (CASSCF) wave function is used for the calculation of PSB3 and MePSB3, respectively. A space composed of six electrons in six π orbitals and state-averaging over three singlet states [SA-3-CASSCF(6,6)] was chosen for computing the orbitals. The reference space for the MR-CIS calculations comprised four electrons in five orbitals [MR-CIS(4,5)], treating the energetically lowest lying π-orbital as reference doubly occupied. Test calculations showed that for PSB3 in total 11 orbitals and for MePSB3 13 lowest doubly occupied orbitals could be frozen in the CI calculation without significant impact on the accuracy of the potential energy surfaces. The 6-31G basis set[54] was selected, since calculations applying this basis set previously reproduce vertical excitation energies, location, and energies of conical intersection and corresponding reaction paths with polarized basis sets exceptionally well[18,21] and reduce the computational cost considerably. In summary, the computational levels are MR-CIS(4,5)-FC11/SA-3-CASSCF(6,6)/6-31G for PSB3 and MR-CIS(4,5)-FC13/SA-3-CASSCF(6,6)/6-31G for MePSB3. Both will be denoted for brevity as MR-CIS(4,5)

Additional comparisons with higher level methods were performed in this work. As benchmark, MR-CI with single and double excitations using the 6-31G(d) basis set and keeping only six orbitals frozen MR-CISD(4,5)-FC6/6-31G(d) was used. The Pople correction[55,56] (denoted as +Q) was added to the energies. For gradients and nonadiabatic coupling vectors these corrections were not available. The level of theory employed finally in the dynamics was tested by comparison of excitation energies, oscillator strengths, energy gradients, nonadiabatic coupling vectors, and character of the wave function for PSB3 including surrounding water molecules represented as point charges for a series of solute/solvent geometries. These geometries were sampled from a nonadiabatic dynamics run and included structures ranging from the initial condition to the crossing seam. Graphs comparing the S_1 excitation energies and the gradients of the dynamics level to the benchmark values can be found in the Supporting Information (comparison of excitation energies, Figure S1, and of excited-state gradients, Figure S2). As can be seen from this comparison, excitation energies and energy gradients agree exceptionally well between the two computational methods throughout the whole trajectory, even in the vicinity of the crossing seam.

dx.doi.org/10.1021/jp400401f | J. Phys. Chem. A 2013, 117, 2790−2799

For the molecular mechanics part of the calculations, the van der Waals parameters, intramolecular parameters, and effective charges were taken from the OPLS/AA force field.[57] For the quantum mechanical part of the calculation, the program system COLUMBUS[58−60] was used. It provides analytic gradients and nonadiabatic coupling vectors for multireference configuration interaction (MRCI).[56,61−64] The implementation of the electrostatic embedding in COLUMBUS is described in ref 46. The molecular mechanics calculations were performed using TINKER.[65] The combination of the hybrid energies and gradients, the integration of the equations of motion and time dependent Schroedinger equation, and the surface hopping were performed using Newton-X.[16,45]

2.2. Setup of the Molecular System, Initial Conditions. The solute (PSB3 or MePSB3) was included in a spherical cluster of either 150 *n*-hexane or 300 water molecules. The initial packing was performed using the PACKMOL program.[66] To keep the gross density at a given value during the dynamics, the entire cluster was included in a spherical boundary for the entire time of the simulation. If an atom crosses the boundary, the radial component of the velocity is reflected (elastic collision). In this way it is ensured that the atom will re-enter the sphere in one of the next time steps or at least will not depart further. The radius of this sphere (15.58 Å for *n*-hexane and 12.95 Å for water) was determined by the condition of maintaining a density of 0.651 g/L for *n*-hexane[67] and 0.997 g/L for water.[67]

A mixed scheme to create initial conditions was employed assigning a Wigner distribution of the quantum mechanical harmonic oscillator[16,68] to the QM atoms ("core atoms") embedded in a set of independent thermalized position/velocity points of the surrounding solvent. The procedure has been described elsewhere.[69] In short, the following steps were adopted:

- The solvent/solute cluster was equilibrated and thermalized at the MM level around the frozen equilibrium structure of the QM region computed for the electronic ground state in gas phase.
- After thermalization, solvent structures were sampled from a ground state trajectory in time steps of 1 ps with the QM region still frozen at the equilibrium structure.
- For the isolated molecule in the QM region initial conditions were calculated using a Wigner distribution.
- The equilibrium QM structure embedded in each of the selected solvent clusters was replaced by a different displaced structure of the Wigner distribution.
- The MM region of each of these sample structures was then rethermalized for 10 ps around its frozen, displaced QM-region structure to adapt the cavity to the new but only slightly modified structure.

Atomic ChelpG[70] charges, used only in the thermalization steps at MM level, were obtained from fitting the electrostatic potential computed at the MRCIS(4,5) level of theory.

2.3. Dynamics Details. Mixed quantum−classical dynamics was performed with on-the-fly calculation of the electronic energies, energy gradients, and nonadiabatic couplings. The nuclear coordinates were treated classically and integrated using the velocity Verlet algorithm[71] with a 0.5 fs time step. Simultaneously, the time-dependent Schrödinger equation was integrated along the classical trajectory by means of the fifth-order Butcher algorithm[72] using a 0.01 fs time step. For this integration, all necessary quantities are interpolated between two classical time steps. To reduce the computational demands, the partial coupling approximation[73] was employed computing only the nonadiabatic couplings including the current state. Decoherence effects were taken into account by the model presented in ref 74 (α = 0.1 hartree). The classical trajectories evolved always on a single adiabatic surface, and the transition probabilities to other surfaces were computed for every 0.01 fs time step by means of the fewest-switches algorithm[75] in the version proposed by Hammes-Schiffer and Tully.[76] In the case of hopping, the momentum excess was adjusted in the direction of the nonadiabatic coupling vectors. In the case of frustrated hopping, the momentum was kept constant.

The nonadiabatic couplings were restricted to the atoms treated fully quantum mechanically (core atoms) by setting the nonadiabatic coupling vector components of the other atoms to zero. This procedure ensures that the nonadiabatic hopping probability is governed only by the quantum mechanically treated region. It also distributes the excess kinetic energy at the time of hopping only to these core atoms, which prevents an unphysical drain of kinetic energy to the solvent after the hopping. For the determination of the possibility of back hopping, only the kinetic energy of the core atoms was taken into consideration. The temperature was kept constant at 298 K using an Anderson thermostat. In order to not interfere with the nonadiabatic treatment, the action of the thermostat was restricted to the solvent molecules.

2.4. Spectra Calculation. Excitation energies and oscillator strengths were calculated at the same level of theory as used for the dynamics simulations. Single-point vertical excitation energies and the corresponding oscillator strengths were computed for all structures created in the course of the preparation of the initial conditions. For the spectral calculation in solution the solvent was included as a set of point charges in the calculations. By use of this information, $S_0 \rightarrow S_1$ absorption spectra were calculated as described in ref 68 using a Lorentzian line shape with a phenomenological broadening, δ, of 0.1 eV. For PSB3 in water, the $S_0 \rightarrow S_2$ absorption spectrum was also calculated using the same parameters.

3. RESULTS AND DISCUSSION

3.1. Spectra. The molecules of the PSB*n* group are known to show a blue shift upon solvation in polar solvents.[12] The relaxed ground state of PSB3 is polar and therefore stabilized by polar solvation, while the excited state in the Franck−Condon region is practically nonpolar and thus less affected by the polar environment.

$S_0 \rightarrow S_1$ absorption spectra of PSB3 in the gas phase, water, and *n*-hexane (Supporting Information Figure S3a) and of MePSB3 in the gas phase and water (Figure S4) and the $S_0 \rightarrow S_2$ spectra of PSB3 in the gas phase and water (Figure S3b) were calculated. Earlier calculations[11] indicate that the S_2 state has a similar charge distribution as the ground state, while in the S_1 a considerable shift of electrons from the carbon tail to the NH_2^+ group is observed. It was therefore of interest to know how the excitation to the second excited state was influenced by polar solvation.

The spectra of both molecules show a pronounced blue shift of the absorption maximum in aqueous solution, +0.32 eV in the case of PSB3 and +0.23 eV in the case of MePSB3. *n*-Hexane has no influence on the position of the absorption maximum. The first excited state is much more strongly destabilized than the second one, which shows no shift in the

absorption maximum with respect to the gas phase. Thus, the S_1-S_2 gap is considerably reduced in polar medium. Indeed, the $S_0 \rightarrow S_1$ and $S_0 \rightarrow S_2$ spectra of PSB3 overlap significantly for aqueous solution in the energy range from 4.75 to 5.50 eV, whereas in the gas phase they are well separated. Because of the overlap of the S_1 and S_2 spectra in aqueous solution, the second excited state was also included in the dynamics in water. However, the analysis of the state occupations performed in the course of the investigations showed that it did not play a significant role in the dynamics.

3.2. Charge Distribution. ChelpG charges were computed at the MR-CIS(4,5) level for 200 structures taken from the initial conditions for the dynamics of PSB3 and MePSB3 in the gas phase and water, respectively. To obtain a simple measure for the overall charge distribution, PSB3 and MePSB3 were divided into two halves with the central double bond as boundary. The "N-side" is the half of the molecule containing the NH_2^+ group, whereas the "C-side" is formed by the other half.

Table 1 lists the charges for the ground and first excited state in the gas phase and in water. For both molecules, vertical

Table 1. ChelpG Charges (e) of PSB3 and MePSB3 in the Ground and in the First Excited State for the Gas Phase and Aqueous Solution[a]

	C-side		N-side	
environment	S_0	S_1	S_0	S_1
		PSB3		
gas phase	0.431	0.513	0.569	0.487
water	0.354	0.484	0.646	0.516
		MePSB3		
gas phase	0.529	0.583	0.471	0.417
water	0.455	0.556	0.545	0.444

[a]See text for definition of C-side and N-side.

excitation to S_1 causes an electron shift from the C-side to the N-side. This shift is stronger for PSB3 than for MePSB3 (gas, 0.082e vs 0.054e; water, 0.130e vs 0.101e); for both molecules, in water the electron shift upon electronic excitation is significantly stronger in comparison to the gas phase. The effect of polar solvation acts in the ground state in the opposite direction than the electronic excitation does: electrons are transferred from the N-side to the C-side. This shift is much stronger in the ground state (PSB3, −0.077e; MePSB3, −0.074e) than in the excited state (PSB3, −0.029e; MePSB3, −0.027e).

Figure 2 shows the development of the charge distribution along sample trajectories of PSB3 in the gas phase and in water and of MePSB3 in water. The overall pattern is identical in all cases. After the initial charge shift with respect to the ground state values due to the electronic excitation, the charge distribution fluctuates around the excited state distribution until the trajectory reaches the vicinity of the crossing seam. There, the electronic structure changes radically between ground and excited state which is accompanied by a transfer of electron density between the two halves of the molecule. After the hopping to the ground state, the electronic density begins to relax back to the original ground state distribution.

3.3. Excited State Lifetimes. In Figure 3, the evolution of the average S_1 population is plotted for all investigated systems. The dynamics starts in S_1 at $t = 0$ and shows a latency time (t_1) during which nearly all trajectories remain in the S_1 state. Only

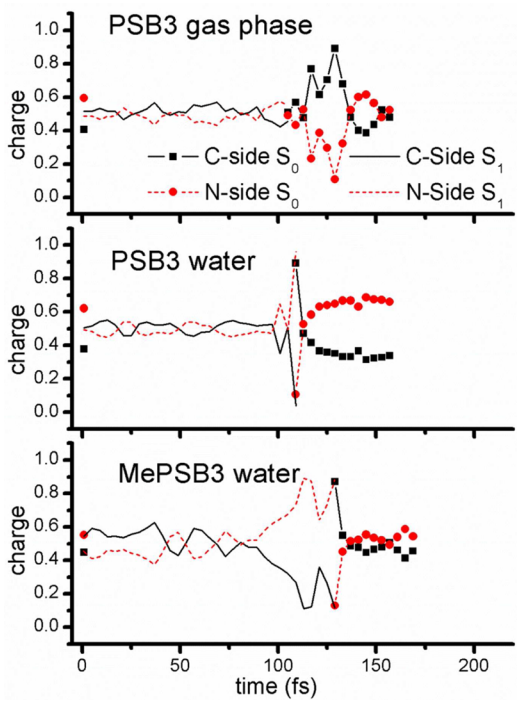

Figure 2. Evolution of the charge density along three sample trajectories for PSB3 in the gas phase (upper panel) and in water (middle panel) and for MePSB3 in water (lower panel). See text for definition of C-side and N-side.

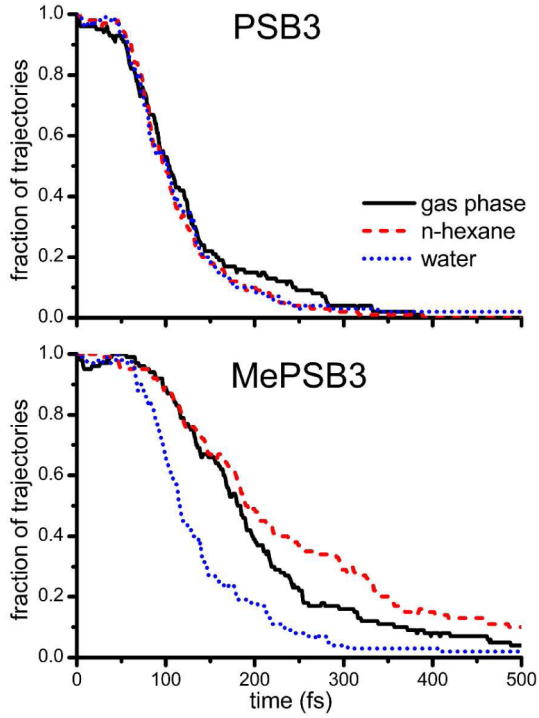

Figure 3. S_1 population for PSB3 (upper panel) and MePSB3 (lower panel) in all environments investigated.

a minor fraction temporarily populates the S_2 state which is neglected in the analysis. When the first trajectories reach the crossing seam, the excited state population begins to decay and the ground state is populated. To determine the excited state

dx.doi.org/10.1021/jp400401f | J. Phys. Chem. A 2013, 117, 2790−2799

lifetime, the S_1 population computed after the onset of the decay is fitted to the function

$$y = y_0 + (1 - y_0)\exp\left(-\frac{(t - t_1)}{t_2}\right)$$

where t_1 is the initial delay or latency time and t_2 is the decay constant. The baseline y_0 was always set to zero, reflecting the assumption of a purely exponential decay with complete depletion of the excited state in the long time limit. The excited-state lifetime (τ) is the sum of t_1 and t_2.

Table 2 lists the lifetimes and averaged hopping parameters (central C−C═C−C torsion, bond length alternation (BLA, difference between the average C−C single bond and C═C double bond lengths)) for all simulated systems. PSB3 shows a latency time of 49−56 fs depending on the environment. The total lifetimes in the gas phase and both solvents are very similar, around 115−128 fs. As shown before,[46] the motion of PSB3 in the excited state is flexible and characterized by rather modest spatial requirements. Therefore, the dynamics is not strongly hindered by steric interaction with solvent molecules.

Table 2. Lifetimes, Average Central C−C═C−C Torsion and BLA at the Time of First Hopping to the Ground State

	time constant				
environment	t_1, fs	t_2, fs	τ, fs	hopping angle, θ (±std dev), deg	hopping BLA (±std dev), Å
PSB3					
gas phase	49	79	128	108 (±25)	−0.016 (±0.071)
n-hexane	56	58	114	110 (±24)	−0.002 (±0.063)
water	51	64	115	111 (±16)	−0.024 (±0.058)
MePSB3					
gas phase	99	110	209	91 (±20)	−0.008 (±0.073)
n-hexane	83	171	254	97 (±19)	−0.014 (±0.063)
water	66	73	139	109 (±12)	−0.019 (±0.064)

For MePSB3, the differences in the excited state lifetime are clearly visible. In the gas phase, MePSB3 has an excited state lifetime of little more than 200 fs, nearly half of it being the latency time t_1. In *n*-hexane, the lifetime is elongated considerably to nearly 260 fs especially because of the increase of t_2. The value of 280 fs reported before[46] was obtained from a simulation without usage of a thermostat for the solvent. The effect of water on the lifetime of MePSB3 is surprising, though. The lifetime is reduced to 139 fs, showing the same behavior in the latency time and the decay constant. So instead of an elongation of the lifetime due to increased steric hindering, the deactivation occurs even more quickly than in the gas phase or in *n*-hexane.

3.4. Collisions with the Solvent. The statistics of close contacts between the solute and the solvent is used to obtain information about steric hindrances. A contact is defined to be close when the distance between two atoms is smaller than the geometric average of their van der Waals radii. The values of the radii (σ-diameter) for PSB3 and MePSB3 were taken from the OPLSAA force field. Where no exact match in atom type could be found, the radius of a similar atom type was used. Table S1 in the Supporting Information lists the parameters used.

Figure 4 shows the number of close contacts of the heavy atoms of PSB3 to heavy atoms of the solvent for both environments. To establish a reference level, adiabatic ground state dynamics simulations were performed for water solution using a set of 20 initial conditions (the same initial conditions as for the excited state). From the number of close contacts one can immediately see that the packing of water molecules is much denser around PSB3 than that of *n*-hexane. Comparison to the ground state dynamics illustrates the effect of the excited state motion. In the nonadiabatic dynamics, an increase in the number of encounters is found especially in the first 60 fs of the dynamics, i.e., in the time the molecule needs to reach the crossing seam. This tendency cannot be seen in the ground-state dynamics where the number of close contacts initially somewhat decreases. Because of the energy gain from the excited state deactivation, starting at about 80−90 fs, PSB3 shows, after switching back to the ground state, a continued hot motion and the number of contacts to the surrounding water molecules remains at a higher level. Relative changes are significantly larger in hexane solution. Longer simulation times, on the order of several picoseconds, would be necessary to distribute the kinetic energy fully to the environment.

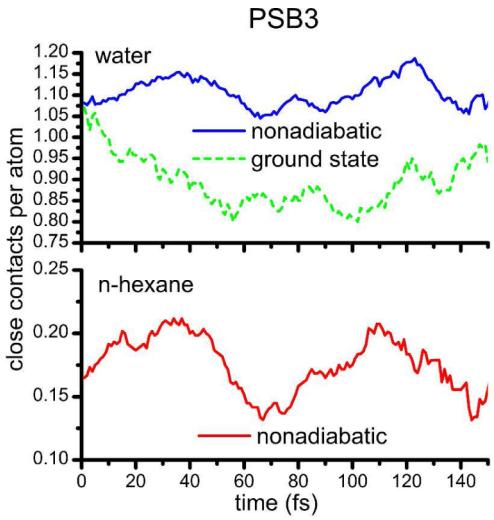

Figure 4. Evolution of the number of close contacts between heavy atoms of the solute and the solvent during the nonadiabatic dynamics for PSB3 in water (upper panel) and in *n*-hexane (lower panel).

As can be seen from Figure 5 for MePSB3, the situation seems to be very similar to PSB3 when considering all heavy solute atoms collectively. When computing the number of contacts for the $-CH_3$ carbon alone, one finds a dominance of this contribution in certain sections of the dynamics, reflecting the torsional motion during the pathway to the crossing seam.

3.5. Geometric Evolution. The general pattern of motions that lead to the crossing seam consists of an adjustment of the bond lengths from the ground state values to those of the excited state and subsequent torsion around the central double bond. This scheme is found to be the same for PSB3 and MePSB3 for all environments. Figure 6 illustrates the BLA of PSB3 and MePSB3 in all investigated media. The evolution of the average BLA is very similar for both molecules and does not change qualitatively in polar or nonpolar solution. It shows a rapid reduction within ~20 fs from the positive ground state value to a larger negative one. Then with oscillations over the next few hundred femtoseconds, the BLA gradually returns to the original level. The initial minimum is deeper in the case of polar solution. This is, however, counterbalanced by a larger rate of increase. Both observations are probably related to the stronger charge shift in water due to the vertical excitation. In

dx.doi.org/10.1021/jp400401f | J. Phys. Chem. A 2013, 117, 2790−2799

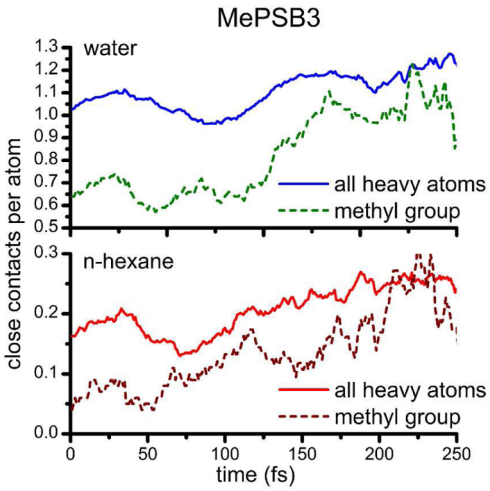

Figure 5. Evolution of the number of close contacts between heavy atoms of the solute and the solvent during the nonadiabatic dynamics for MePSB3 in water (upper panel) and in *n*-hexane (lower panel). Results for the $-CH_3$ group are plotted separately.

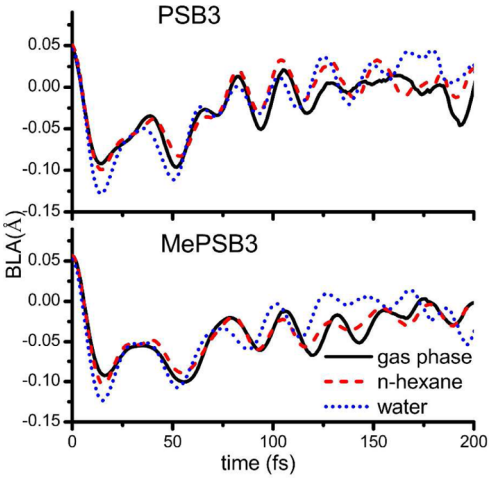

Figure 6. Evolution of the BLA value for PSB3 (upper panel) and MePSB3 (lower panel) for all simulated environments.

PSB3, therefore, the zero level is reached in about the same time for water as for the gas phase and *n*-hexane. For MePSB3, where the increase takes longer, the water-solvated system reaches the zero line even a bit earlier than in the gas phase or *n*-hexane. It should be noted that in water the average BLA at the time of first hopping is shifted for both molecules to more negative numbers (see Table 2).

Figure 7 and Figure 8 display the central torsional angles of all trajectories for PSB3 and MePSB3, respectively. The points of first hopping to the ground state are marked by black dots. Already in the gas phase, the two molecules behave differently. The torsion of PSB3 passes the conical intersection and leaves the vicinity of the intersection seam rapidly. Because of the substitution of the central double bond ($-CH_3$ vs $-H$), MePSB3 shows a tendency to stay longer in the vicinity of the crossing seam before the trajectory changes into the ground state.

Neither water nor *n*-hexane solvation changes the general behavior of the torsional dynamics of PSB3. As discussed before,[46] the torsional motion of PSB3 that leads to the crossing seam is very space-efficient and flexible and is not

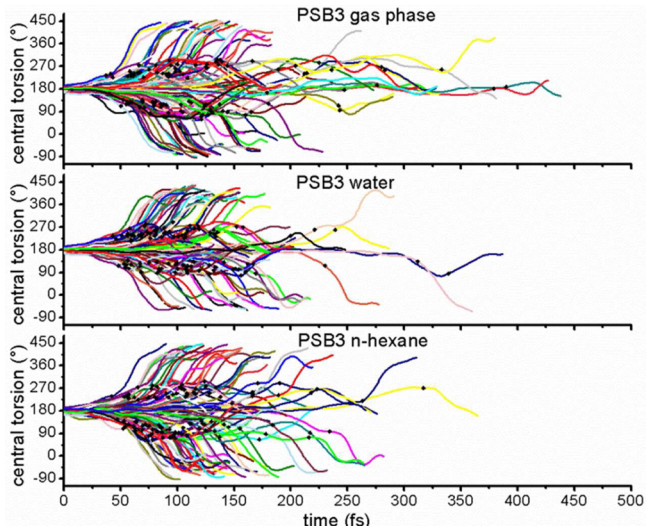

Figure 7. Evolution of the central torsional angle of PSB3 in the gas phase (upper panel), water (middle panel), and *n*-hexane (lower panel). The points of hopping are marked with dots.

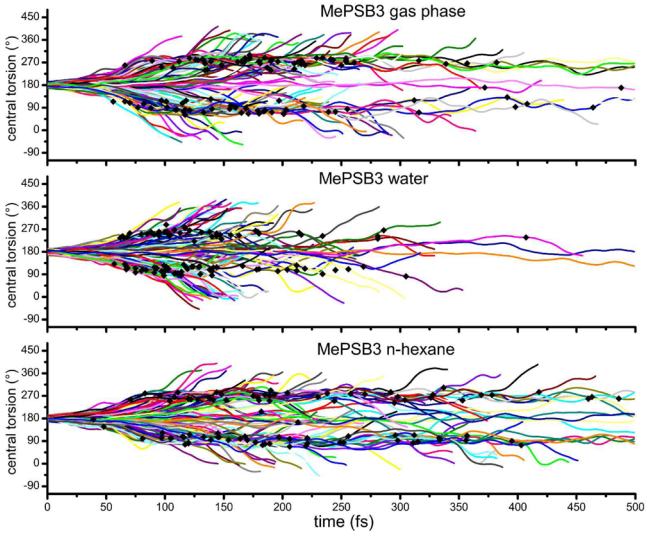

Figure 8. Evolution of the central torsional angle of MePSB3 in the gas phase (upper panel), water (middle panel), and *n*-hexane (lower panel). The points of hopping are marked with dots.

easily impeded by mechanical restrictions. The excited state torsion of MePSB3 is not so fast. The additional mass of the $-CH_3$ group on one side of the molecule shifts the major portion of the torsional motion to the other side. Additionally, the bulky methyl group sticking out from the molecular axis acts as an anchor in the environment, thus limiting even further the mobility of one-half of the molecule.

Because of the C_s symmetry of the PSB3 and MePSB3 ground state minimum, the central torsion is equally probable in both directions. In the following analysis the central torsional angles observed in the trajectories are folded into the range between 180° (trans) and 0° (cis). Figure 9 shows the time evolution of the averaged absolute central torsional angle for PSB3 and MePSB3, respectively, in all simulated environments. The hindrance of the torsional motion of PSB3 in water is observed in the later phase of the dynamics; the presence of *n*-hexane does not affect the PSB3 motion significantly. MePSB3 is visibly impeded in its torsional motion, the obstruction being

dx.doi.org/10.1021/jp400401f | J. Phys. Chem. A 2013, 117, 2790−2799

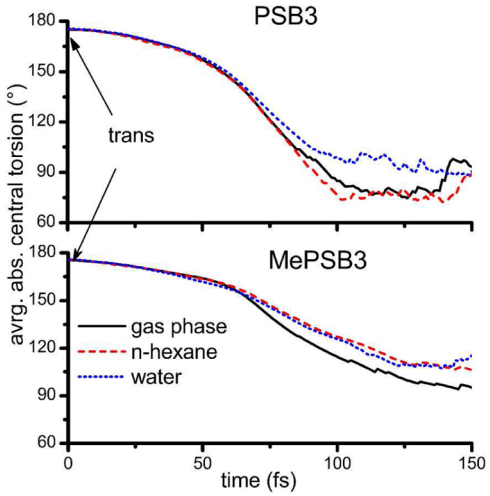

Figure 9. Evolution of the central torsional angle averaged over all trajectories for PSB3 (upper panel) and MePSB3 (lower panel). All values are folded into the range of 0° (cis) to 180° (trans).

the same in *n*-hexane and water. In view of this fact, the reduction of its lifetime in aqueous solution is surprising. At the same time, the average hopping angle is not shifted very much to the trans-side for MePSB3 in hexane, as can be seen from Table 2.

3.6. The Crossing Seam. The effect of polar solvation on the spectrum suggests that in water the crossing seam is altered also. This assumption is reasonable when regarding the strong stabilization of the ground state relative to the first excited state in the Franck−Condon region. Indeed, Burghardt et al., on the basis of a PSB3 model including continuum solvation with variable polarization, have shown[31,51,52] that the crossing seam of PSB3 will, when exposed to a polarizing field, be shifted or, in the extreme case, could vanish completely. The coordinate along which the crossing seam was shifted in their model was the central C═C stretch. This coordinate is closely related to the BLA, and therefore, this is the direction for searching for a shift of the crossing seam in our calculations.

The minimum of the crossing seam (MXS) has been optimized for PSB3 and MePSB3 in the gas phase at the computational level of the dynamics simulation (MR-CIS-(4,5)). The two vectors spanning the intersection subspace (gradient difference vector (**g**) and nonadiabatic coupling vector (**h**)) consist mainly of components related to bond length changes and the central torsion, respectively. To estimate the location and structure of the crossing seam in solution, the points of hopping with ΔE_{hop} lower than 0.5 eV were collected from all trajectories computed for water as solvent and, freezing the respective solvent geometry, an optimization of the MXS was performed within the field of the solvent point charges. This procedure was carried out for 13 representative structures of PSB3 and for 8 structures of MePSB3. The BLA values of the gas phase MXS and the averaged values for the water-solvated structures are given in Table 3. For both PSB3 and MePBS3, the BLA is shifted to smaller values by inclusion of the aqueous environment compared to the gas phase, the shift being larger for MePSB3. This is consistent with the trend obtained from the average BLA at the point of first hopping (Table 2) for the gas phase and water. Figure 6 shows that the crossing seam is reached in an upward trend with respect to the BLA starting

Table 3. BLA and Central Torsion for MXS Structures

environment (no. struct)	BLA (±std dev), Å	θ (±std dev), deg
	PSB3	
gas phase	−0.011	87
water (13)	−0.031 (±0.004)	98 (±3)
	MePSB3	
gas phase	0.009	107
water (8)	−0.027 (±0.011)	94 (±7)

from negative BLA values. Thus, a more negative value of the BLA for the MXS means that the crossing seam is reached earlier in time in the dynamics. The difference between BLA values for the gas phase and water is one of the reasons for the speedup of the excited state deactivation in polar solution. This difference is more pronounced for MePSB3 in water, for which the critical MXS value is reached much earlier than in the gas phase. For PSB3 this effect is not as important.

Solvation effects not only affect the molecular structure at the MXS but also the topology of the cone, which subsequently will also change the efficiency of the deactivation to the ground state. Figures S5 and S6 (Supporting Information) display the cones for PSB3 in the gas phase and for one selected solvent distribution. The conical intersection in the gas phase is sloped in the direction of the gradient difference vector, whereas in aqueous solution the cone is peaked. This fact should lead to a higher efficiency of the conversion to the ground state.[77] In Table 4, the average time per trajectory in the excited state near

Table 4. Average Time of a Trajectory in the Excited State near the Crossing Seam

environment	av time, fs
PSB3	
gas phase	30
n-hexane	32
water	16
MePSB3	
gas phase	95
n-hexane	133
water	26

the crossing seam is displayed. A trajectory was considered to be near the crossing seam from the moment the energy difference between S_0 and S_1 was less than 0.5 eV till it either changed to the ground state or left the region of the seam (the energy difference increased above 1.2 eV). Table 4 shows that this time is much shorter for both molecules in water. Moreover, the effect is significantly larger for MePSB3. Closer analysis shows that the major part of this speedup is caused by the fact that the trajectories in the gas phase and *n*-hexane frequently approach the crossing seam more than one time before changing to the ground state while in water almost all trajectories are deactivated at the first attempt. This accounts for the major part of the difference in lifetime in MePSB3.

4. CONCLUSIONS

The photodynamics of the retinal model systems *all-trans*-2,4-pentadiene-iminium cation (protonated Schiff base 3, PSB3) and the *all-trans*-3-methyl-2,4-pentadiene-iminium cation (MePSB3) have been investigated in the gas phase and in nonpolar (*n*-hexane) and polar (water) solvation using an MRCI-QM/MM approach. Because of its structural flexibility,

dx.doi.org/10.1021/jp400401f | J. Phys. Chem. A 2013, 117, 2790−2799

the computed lifetime of PSB3 is not affected much by the presence of a solvent. Substituting PSB3 with a methyl group impedes the torsional motion substantially in the gas phase, which leads to a significant enhancement of the MePSB3 lifetime in the gas phase and in nonpolar solution. However, its lifetime is reduced significantly in aqueous solution and is even considerably smaller than in the gas phase.

Several factors characterizing electronic and steric properties in the course of the dynamics of PSB3 and PSB3 have been investigated systematically. As the most important factor, the influence of the polar environment on the intersection seam has been identified: in aqueous solution the crossing seam is shifted such that the molecules reach the vicinity of the crossing seam earlier than in the gas phase. This is in line with earlier proposals by Burghardt and Hynes based on their model studies.[26,46,47] Moreover, the intersection cone is sloped in the gas phase but peaked in aqueous solution. This fact is mainly responsible for the increase of the efficiency of the excited state deactivation in polar solution. The combination of the shift of the intersection seam and the characteristics of the cone can accelerate the decay of the excited state considerably.

For PSB3, the deactivation is quite efficient from the beginning and the speedup gained by the shift of the crossing seam merely compensates for the steric hindering in water. In the case of MePSB3 the photodynamics proceeds at a slower scale and the changes in the properties of the intersection seam toward earlier access in the dynamics and improved efficiency lead to a significant reduction of the lifetime in water that is much shorter even than in the gas phase. This example demonstrates explicitly the general role a polar environment can play and the necessity to include it in the quantum mechanical calculations when performing nonadiabatic dynamics.

■ ASSOCIATED CONTENT

Supporting Information

Graphs comparing different levels of theory, simulated spectra, conical intersection shapes, and Lennard-Jones parameters. This material is available free of charge via the Internet at http://pubs.acs.org.

■ AUTHOR INFORMATION

Corresponding Author

*For H.L.: e-mail, hans.lischka@univie.ac.at. For M.B.: e-mail, barbatti@kofo.mpg.de.

Present Address

[⊥]For M.R.: Institute for Physical and Theoretical Chemistry, Goethe University Frankfurt, Max-von-Laue-Strasse 7, 60438 Frankfurt am Main, Germany.

Notes

The authors declare no competing financial interest.

■ ACKNOWLEDGMENTS

We thank Prof. Dr. Irene Burghardt for her valuable input in the discussion of the solvent effect on the crossing seam. Part of the final work (M.R.) has been performed in her work group at Goethe University, Frankfurt am Main, Germany. This work was supported by the Austrian Science Fund within the framework of the Special Research Program F41 (ViCoM). Support was provided by the Robert A.Welch Foundation under Grant No. D-0005. The authors also thank, for technical support and computer time, the VSC—Vienna Scientific Cluster (Project Nos. 70019 and 70151). Displays of molecular structures were made with VMD. VMD is developed with NIH support by the Theoretical and Computational Biophysics group at the Beckman Institute, University of Illinois at Urbana-Champaign (http://www.ks.uiuc.edu/Research/vmd/).

■ REFERENCES

(1) Birge, R. R. Nature of the Primary Photochemical Events in Rhodopsin and Bacteriorhodopsin. *Biochim. Biophys. Acta* **1990**, *1016*, 293−327.

(2) Schoenlein, R. W.; Peteanu, L. A.; Mathies, R. A.; Shank, C. V. The 1st Step in Vision—Femtosecond Isomerization of Rhodopsin. *Science* **1991**, *254*, 412−415.

(3) Palings, I.; Pardoen, J. A.; Vandenberg, E.; Winkel, C.; Lugtenburg, J.; Mathies, R. A. Assignment of Fingerprint Vibrations in the Resonance Raman-Spectra of Rhodopsin, Isorhodopsin, and Bathorhodopsin—Implications for Chromophore Structure and Environment. *Biochemistry* **1987**, *26*, 2544−2556.

(4) Altoe, P.; Cembran, A.; Olivucci, M.; Garavelli, M. Aborted Double Bicycle-Pedal Isomerization with Hydrogen Bond Breaking Is the Primary Event of Bacteriorhodopsin Proton Pumping. *Proc. Natl. Acad. Sci. U.S.A.* **2010**, *107*, 20172−20177.

(5) Polli, D.; Altoe, P.; Weingart, O.; Spillane, K. M.; Manzoni, C.; Brida, D.; Tomasello, G.; Orlandi, G.; Kukura, P.; Mathies, R. A.; et al. Conical Intersection Dynamics of the Primary Photoisomerization Event in Vision. *Nature* **2010**, *467*, 440−443.

(6) Warshel, A. Bicycle-Pedal Model for 1st Step in Vision Process. *Nature* **1976**, *260*, 679−683.

(7) Liu, R. S. H.; Mead, D.; Asato, A. E. Photochemistry of Polyenes. 23. Application of the H.T.-N Mechanism of Photoisomerization to the Photocycles of Bacteriorhodopsin—A Model Study. *J. Am. Chem. Soc.* **1985**, *107*, 6609−6614.

(8) Liu, R. S. H.; Hammond, G. S. Examples of Hula-Twist in Photochemical Cis−Trans Isomerization. *Chem.—Eur. J.* **2001**, *7*, 4536−4544.

(9) Schapiro, I.; Ryazantsev, M. N.; Frutos, L. M.; Ferre, N.; Lindh, R.; Olivucci, M. The Ultrafast Photoisomerizations of Rhodopsin and Bathorhodopsin Are Modulated by Bond Length Alternation and HOOP Driven Electronic Effects. *J. Am. Chem. Soc.* **2011**, *133*, 3354−3364.

(10) Migani, A.; Robb, M. A.; Olivucci, M. Relationship between Photoisomerization Path and Intersection Space in a Retinal Chromophore Model. *J. Am. Chem. Soc.* **2003**, *125*, 2804−2808.

(11) Cembran, A.; Bernardi, F.; Olivucci, M.; Garavelli, M. Counterion Controlled Photoisomerization of Retinal Chromophore Models: A Computational Investigation. *J. Am. Chem. Soc.* **2004**, *126*, 16018−16037.

(12) Wanko, M.; Hoffmann, M.; Strodet, P.; Koslowski, A.; Thiel, W.; Neese, F.; Frauenheim, T.; Elstner, M. Calculating Absorption Shifts for Retinal Proteins: Computational Challenges. *J. Phys. Chem. B* **2005**, *109*, 3606−3615.

(13) Sumita, M.; Saito, K. Theoretical Study on Hula-Twist Motion of Penta-2,4-dieniminium on the S_1 Surface under Isolated Condition by the Complete Active Space Self-Consistent Field Theory. *Chem. Phys. Lett.* **2006**, *424*, 374−378.

(14) Send, R.; Sundholm, D. Stairway to the Conical Intersection: A Computational Study of the Retinal Isomerization. *J. Phys. Chem. A* **2007**, *111*, 8766−8773.

(15) Weingart, O.; Schapiro, I.; Buss, V. Photochemistry of Visual Pigment Chromophore Models by ab Initio Molecular Dynamics. *J. Phys. Chem. B* **2007**, *111*, 3782−3788.

(16) Barbatti, M.; Granucci, G.; Persico, M.; Ruckenbauer, M.; Vazdar, M.; Eckert-Maksic, M.; Lischka, H. The On-the-Fly Surface-Hopping Program System Newton-X: Application to ab Initio Simulation of the Nonadiabatic Photodynamics of Benchmark Systems. *J. Photochem. Photobiol., A* **2007**, *190*, 228−240.

(17) Barbatti, M.; Ruckenbauer, M.; Szymczak, J. J.; Aquino, A. J. A.; Lischka, H. Nonadiabatic Excited-State Dynamics of Polar Π-Systems

and Related Model Compounds of Biological Relevance. *Phys. Chem. Chem. Phys.* **2008**, *10*, 482−494.
(18) Szymczak, J. J.; Barbatti, M.; Lischka, H. Mechanism of Ultrafast Photodecay in Restricted Motions in Protonated Schiff Bases: The Pentadieniminium Cation. *J. Chem. Theory Comput.* **2008**, *4*, 1189−1199.
(19) Garavelli, M.; Celani, P.; Bernardi, F.; Robb, M. A.; Olivucci, M. The $C_5H_6NH_2^+$ Protonated Shiff Base: An ab Initio Minimal Model for Retinal Photoisomerization. *J. Am. Chem. Soc.* **1997**, *119*, 6891−6901.
(20) Aquino, A. J. A.; Barbatti, M.; Lischka, H. Excited-State Properties and Environmental Effects for Protonated Schiff Bases: A Theoretical Study. *ChemPhysChem* **2006**, *7*, 2089−2096.
(21) Szymczak, J. J.; Barbatti, M.; Lischka, H. Is the Photoinduced Isomerization in Retinal Protonated Schiff Bases a Single- or Double-Torsional Process? *J. Phys. Chem. A* **2009**, *113*, 11907−11918.
(22) Keal, T. W.; Wanko, M.; Thiel, W. Assessment of Semiempirical Methods for the Photoisomerisation of a Protonated Schiff Base. *Theor. Chem. Acc.* **2009**, *123*, 145−156.
(23) Mori, T.; Nakano, K.; Kato, S. Conical Intersections of Free Energy Surfaces in Solution: Effect of Electron Correlation on a Protonated Schiff Base in Methanol Solution. *J. Chem. Phys.* **2010**, *133*, 064107.
(24) Valsson, O.; Filippi, C. Photoisomerization of Model Retinal Chromophores: Insight from Quantum Monte Carlo and Multiconfigurational Perturbation Theory. *J. Chem. Theory Comput.* **2010**, *6*, 1275−1292.
(25) Gozem, S.; Huntress, M.; Schapiro, I.; Lindh, R.; Granovsky, A. A.; Angeli, C.; Olivucci, M. Dynamic Electron Correlation Effects on the Ground State Potential Energy Surface of a Retinal Chromophore Model. *J. Chem. Theory Comput.* **2012**, *8*, 4069−4080.
(26) Klaffki, N.; Weingart, O.; Garavelli, M.; Spohr, E. Sampling Excited State Dynamics: Influence of HOOP Mode Excitations in a Retinal Model. *Phys. Chem. Chem. Phys.* **2012**, *14*, 14299−14305.
(27) Bakowies, D.; Thiel, W. Hybrid Models for Combined Quantum Mechanical and Molecular Mechanical Approaches. *J. Phys. Chem.* **1996**, *100*, 10580−10594.
(28) Sherwood, P. Hybrid Quantum Mechanics/Molecular Mechanics. In *Modern Methods and Algorithms of Quantum Chemistry*; Grotendorst, J., Ed.; John von Neumann Institute for Computing: Jülich, Germany, 2000; Vol. 3; pp 285−305.
(29) Lin, H.; Truhlar, D. G. QM/MM: What Have We Learned, Where Are We, and Where Do We Go from Here? *Theor. Chem. Acc.* **2007**, *117*, 185−199.
(30) Saam, J.; Tajkhorshid, E.; Hayashi, S.; Schulten, K. Molecular Dynamics Investigation of Primary Photoinduced Events in the Activation of Rhodopsin. *Biophys. J.* **2002**, *83*, 3097−3112.
(31) Burghardt, I.; Cederbaum, L. S.; Hynes, J. T. Environmental Effects on a Conical Intersection: A Model Study. *Faraday Discuss.* **2004**, *127*, 395−411.
(32) Rohrig, U. F.; Guidoni, L.; Laio, A.; Frank, I.; Rothlisberger, U. A Molecular Spring for Vision. *J. Am. Chem. Soc.* **2004**, *126*, 15328−15329.
(33) Sekharan, S.; Sugihara, M.; Buss, V. Origin of Spectral Tuning in Rhodopsin—It Is Not the Binding Pocket. *Angew. Chem., Int. Ed.* **2007**, *46*, 269−271.
(34) Warshel, A.; Chu, Z. T. Nature of the Surface Crossing Process in Bacteriorhodopsin: Computer Simulations of the Quantum Dynamics of the Primary Photochemical Event. *J. Phys. Chem. B* **2001**, *105*, 9857−9871.
(35) Hoffmann, M.; Wanko, M.; Strodel, P.; Konig, P. H.; Frauenheim, T.; Schulten, K.; Thiel, W.; Tajkhorshid, E.; Elstner, M. Color Tuning in Rhodopsins: The Mechanism for the Spectral Shift between Bacteriorhodopsin and Sensory Rhodopsin II. *J. Am. Chem. Soc.* **2006**, *128*, 10808−10818.
(36) Toniolo, A.; Granucci, G.; Martínez, T. J. Conical Intersections in Solution: A QM/MM Study Using Floating Occupation Semiempirical Configuration Interaction Wave Functions. *J. Phys. Chem. A* **2003**, *107*, 3822−3830.
(37) Groenhof, G.; Bouxin-Cademartory, M.; Hess, B.; deVisser, S. P.; Berendsen, H. J. C.; Olivucci, M.; Mark, A. E.; Robb, M. A. Photoactivation of the Photoactive Yellow Protein: Why Photon Absorption Triggers a Trans-to-Cis Isomerization of the Chromophore in the Protein. *J. Am. Chem. Soc.* **2004**, *126*, 4228−4233.
(38) Frutos, L. M.; Andruniow, T.; Santoro, F.; Ferre, N.; Olivucci, M. Tracking the Excited-State Time Evolution of the Visual Pigment with Multiconfigurational Quantum Chemistry. *Proc. Natl. Acad. Sci. U.S.A.* **2007**, *104*, 7764−7769.
(39) Ciminelli, C.; Granucci, G.; Persico, M. The Photoisomerization of a Peptidic Derivative of Azobenzene: A Nonadiabatic Dynamics Simulation of a Supramolecular System. *Chem. Phys.* **2008**, *349*, 325−333.
(40) Hayashi, S.; Taikhorshid, E.; Schulten, K. Photochemical Reaction Dynamics of the Primary Event of Vision Studied by Means of a Hybrid Molecular Simulation. *Biophys. J.* **2009**, *96*, 403−416.
(41) Zhenggang, L.; You, L.; Fabiano, E.; Thiel, W. QM/MM Nonadiabatic Decay Dynamics of 9*H*-Adenine in Aqueous Solution. *ChemPhysChem* **2011**, *12*, 1989−1998.
(42) Levine, B. G.; Coe, J. D.; Virshup, A. M.; Martinez, T. J. Implementation of ab Initio Multiple Spawning in the Molpro Quantum Chemistry Package. *Chem. Phys.* **2008**, *347*, 3−16.
(43) Bockmann, M.; Doltsinis, N. L.; Marx, D. Nonadiabatic Hybrid Quantum and Molecular Mechanic Simulations of Azobenzene Photoswitching in Bulk Liquid Environment. *J. Phys. Chem. A* **2010**, *114*, 745−754.
(44) Virshup, A. M.; Punwong, C.; Pogorelov, T. V.; Lindquist, B. A.; Ko, C.; Martinez, T. J. Photodynamics in Complex Environments: Ab Initio Multiple Spawning Quantum Mechanical/Molecular Mechanical Dynamics. *J. Phys. Chem. B* **2009**, *113*, 3280−3291.
(45) Barbatti, M.; Lischka, H.; Granucci, G.; Persico, M.; Ruckenbauer, M.; Pittner, J.; Plasser, F. Newton-X: A Package for Newtonian Dynamics Close to the Crossing Seam. www.newtonx.org (2011).
(46) Ruckenbauer, M.; Barbatti, M.; Muller, T.; Lischka, H. Nonadiabatic Excited-State Dynamics with Hybrid ab Initio Quantum-Mechanical/Molecular-Mechanical Methods: Solvation of the Pentadieniminium Cation in Apolar Media. *J. Phys. Chem. A* **2010**, *114*, 6757−6765.
(47) Nachtigallova, D.; Zeleny, T.; Ruckenbauer, M.; Muller, T.; Barbatti, M.; Hobza, P.; Lischka, H. Does Stacking Restrain the Photodynamics of Individual Nucleobases? *J. Am. Chem. Soc.* **2010**, *132*, 8261−8263.
(48) Zeleny, T.; Hobza, P.; Nachtigallova, D.; Ruckenbauer, M.; Lischka, H. Photodynamics of the Adenine Model 4-Aminopyrimidine Embedded within Double Strand of DNA. *Collect. Czech. Chem. Commun.* **2011**, *76*, 631−643.
(49) Zeleny, T.; Ruckenbauer, M.; Aquino, A. J. A.; Muller, T.; Lankas, F.; Drsata, T.; Hase, W. L.; Nachtigallova, D.; Lischka, H. Strikingly Different Effects of Hydrogen Bonding on the Photodynamics of Individual Nucleobases in DNA: Comparison of Guanine and Cytosine. *J. Am. Chem. Soc.* **2012**, *134*, 13662−13669.
(50) Eckert-Maksic, M.; Vazdar, M.; Ruckenbauer, M.; Barbatti, M.; Muller, T.; Lischka, H. Matrix-Controlled Photofragmentation of Formamide: Dynamics Simulation in Argon by Nonadiabatic QM/MM Method. *Phys. Chem. Chem. Phys.* **2010**, *12*, 12719−12726.
(51) Burghardt, I.; Hynes, J. T. Excited-State Charge Transfer at a Conical Intersection: Effects of an Environment. *J. Phys. Chem. A* **2006**, *110*, 11411−11423.
(52) Spezia, R.; Burghardt, I.; Hynes, J. T. Conical Intersections in Solution: Non-Equilibrium versus Equilibrium Solvation. *Mol. Phys.* **2006**, *104*, 903−914.
(53) Szalay, P. G.; Muller, T.; Gidofalvi, G.; Lischka, H.; Shepard, R. Multiconfiguration Self-Consistent Field and Multireference Configuration Interaction Methods and Applications. *Chem. Rev.* **2012**, *112*, 108−181.
(54) Hehre, W. J.; Ditchfield, R.; Pople, J. A. Self-Consistent Molecular-Orbital Methods. 12. Further Extensions of Gaussian-Type

Basis Sets for Use in Molecular-Orbital Studies of Organic-Molecules. *J. Chem. Phys.* **1972**, *56*, 2257−2261.
(55) Pople, J. A.; Seeger, R.; Krishnan, R. Variational Configuration Interaction Methods and Comparison with Perturbation-Theory. *Int. J. Quantum Chem.* **1977**, 149−163.
(56) Shepard, R. The Analytic Gradient Method for Configuration Interaction Wave Functions. In *Modern Electronic Structure Theory*; Yarkony, D. R., Ed.; World Scientific: Singapore, 1995; Vol. *1*, p 345.
(57) Jorgensen, W. L.; McDonald, N. A. Development of an All-Atom Force Field for Heterocycles. Properties of Liquid Pyridine and Diazenes. *THEOCHEM: J. Mol. Struct.* **1998**, *424*, 145−155.
(58) Lischka, H.; Shepard, R.; Pitzer, R. M.; Shavitt, I.; Dallos, M.; Müller, T.; Szalay, P. G.; Seth, M.; Kedziora, G. S.; Yabushita, S.; et al. High-Level Multireference Methods in the Quantum-Chemistry Program System Columbus: Analytic MR-CISD and MR-AQCC Gradients and MR-AQCC-LRT for Excited States, GUGA Spin-Orbit CI and Parallel CI Density. *Phys. Chem. Chem. Phys.* **2001**, *3*, 664−673.
(59) Lischka, H.; Shepard, R.; Shavitt, I.; Pitzer, R. M.; Dallos, M.; Mueller, T.; Szalay, P. G.; Brown, F. B.; Ahlrichs, R.; Boehm, H. J.; et al.et al. COLUMBUS, an ab Initio Electronic Structure Program, release 7.0; 2012.
(60) Lischka, H.; Shepard, R.; Brown, F. B.; Shavitt, I. New Implementation of the Graphical Unitary-Group Approach for Multi-Reference Direct Configuration-Interaction Calculations. *Int. J. Quantum Chem.* **1981**, *S15*, 91−100.
(61) Dallos, M.; Lischka, H.; Shepard, R.; Yarkony, D. R.; Szalay, P. G. Analytic Evaluation of Nonadiabatic Coupling Terms at the MR-CI Level. II. Minima on the Crossing Seam: Formaldehyde and the Photodimerization of Ethylene. *J. Chem. Phys.* **2004**, *120*, 7330−7339.
(62) Lischka, H.; Dallos, M.; Shepard, R. Analytic MRCI Gradient for Excited States: Formalism and Application to the n-pi* Valence- and n-(3s,3p) Rydberg States of Formaldehyde. *Mol. Phys.* **2002**, *100*, 1647−1658.
(63) Lischka, H.; Dallos, M.; Szalay, P. G.; Yarkony, D. R.; Shepard, R. Analytic Evaluation of Nonadiabatic Coupling Terms at the MR-CI Level. I. Formalism. *J. Chem. Phys.* **2004**, *120*, 7322−7329.
(64) Shepard, R.; Lischka, H.; Szalay, P. G.; Kovar, T.; Ernzerhof, M. A General Multireference Configuration-Interaction Gradient Program. *J. Chem. Phys.* **1992**, *96*, 2085−2098.
(65) Ponder, J. W.; Richards, F. M. An Efficient Newton-like Method for Molecular Mechanics Energy Minimization of Large Molecules. *J. Comput. Chem.* **1987**, *8*, 1016−1024.
(66) Martínez, L.; A., R.; Birgin, E. G.; Martínez., J. M. Packmol: A Package for Building Initial Configurations for Molecular Dynamics Simulations. *J. Comput. Chem.* **2009**, *30*, 2157−2164.
(67) D'Ans, L. *Taschenbuch für Chemiker und Physiker*; Springer Verlag: Berlin, Heidelberg, New York, 1967; Vol. *1*.
(68) Barbatti, M.; Aquino, A. J. A.; Lischka, H. The UV Absorption of Nucleobases: Semi-Classical ab Initio Spectra Simulations. *Phys. Chem. Chem. Phys.* **2010**, *12*, 4959−67.
(69) Sellner, B.; Ruckenbauer, M.; Stambolic, I.; Barbatti, M.; Aquino, A. J. A.; Lischka, H. Photodynamics of Azomethane: A Nonadiabatic Surface-Hopping Study. *J. Phys. Chem. A* **2010**, *114*, 8778−8785.
(70) Breneman, C. M.; Wiberg, K. B. Determining Atom-Centered Monopoles from Molecular Electrostatic Potentials—The Need for High Sampling Density in Formamide Conformational Analysis. *J. Comput. Chem.* **1990**, *11*, 361−373.
(71) Swope, W. C.; Andersen, H. C.; Berens, P. H.; Wilson, K. R. A Computer-Simulation Method for the Calculation of Equilibrium-Constants for the Formation of Physical Clusters of Molecules—Application to Small Water Clusters. *J. Chem. Phys.* **1982**, *76*, 637−649.
(72) Butcher, J. *J. Assoc. Comput. Mach.* **1965**, *12*, 124−135.
(73) Pittner, J.; Lischka, H.; Barbatti, M. Optimization of Mixed Quantum-Classical Dynamics: Time-Derivative Coupling Terms and Selected Couplings. *Chem. Phys.* **2009**, *356*, 147−152.
(74) Granucci, G.; Persico, M. Critical Appraisal of the Fewest Switches Algorithm for Surface Hopping. *J. Chem. Phys.* **2007**, *126*, 134114 1−11.
(75) Tully, J. C. Molecular-Dynamics with Electronic-Transitions. *J. Chem. Phys.* **1990**, *93*, 1061−1071.
(76) Hammes-Schiffer, S.; Tully, J. C. Proton-Transfer in Solution—Molecular-Dynamics with Quantum Transitions. *J. Chem. Phys.* **1994**, *101*, 4657−4667.
(77) Atchity, G. J.; Xantheas, S. S.; Ruedenberg, K. Potential-Energy Surfaces near Intersections. *J. Chem. Phys.* **1991**, *95*, 1862−1876.